ACS OMEGA

http://pubs.acs.org/journal/acsodf

Article

Hydroxyapatite Fabrication for Enhancing Biohydrogen Production from Glucose Dark Fermentation

Haoe Mo, Na Wang, Zhongmin Ma, Jishi Zhang, Jinlong Zhang, Lu Wang, Weifang Dong,* and Lihua Zang*

Cite This: *ACS Omega* 2022, 7, 10550−10558

Read Online

ACCESS | Metrics & More | Article Recommendations | Supporting Information

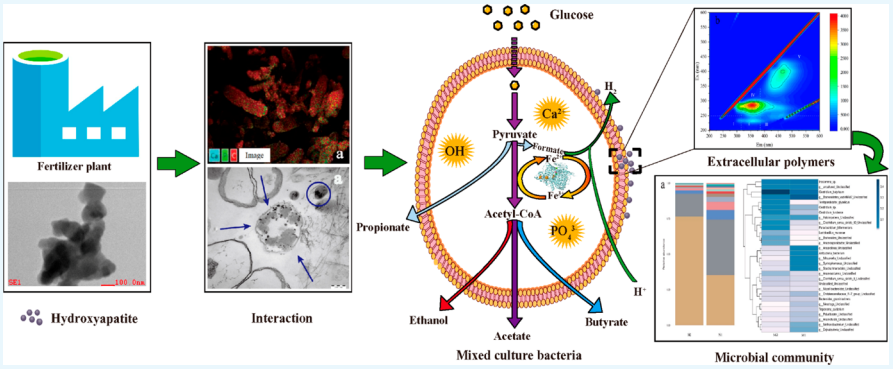

ABSTRACT: Hydroxyapatite (HA) had the effect of maintaining the pH balance of the reaction system and promoting enzyme activity. In this work, hydroxyapatite was synthesized by coprecipitation and characterized for biohydrogen ($bioH_2$) production from glucose. The highest $bioH_2$ yield obtained was 182.33 ± 2.41 mL/g glucose, amended with an optimal dosage of 400 mg/L HA, which was a 55.80% higher $bioH_2$ yield compared with the control group without any addition. The results indicated that HA facilitated the deterioration of organic substances and increased the concentration of soluble microbial products (SMPs). Microbial community analysis revealed that HA significantly increased the abundance of *Firmicutes* from 35.27% (0 mg/L, HA) to 76.41% (400 mg/L, HA), which played an essential role in $bioH_2$ generation. In particular, the abundance of *Clostridium sensu stricto 1* increased from 15.33% (0 mg/L HA) to 45.17% (400 mg/L HA) and became the dominant bacteria. The results also indicated that HA likely improves $bioH_2$ production from organic wastewater in practice.

1. INTRODUCTION

Energy is the basis for society's progress and mankind's existence and is mainly derived from fossil fuels.[1] The limitations of fossil energy sources and the environmental problems associated with fossil energy combustion are driving an increasing interest in the use of biofuels such as biohydrogen ($bioH_2$) and ethanol (EtOH) as alternative energy sources for transportation.[2] Furthermore, $bioH_2$ has a higher energy mass content compared to other fuels and can be produced from renewable substrates such as straw, waste sludge, and high concentrations of chemical oxygen demand (COD).[3]

Various approaches have been used to fabricate $bioH_2$, including photoderived and dark fermentations. Dark fermentation is considered an efficient process and provides an attractive and environmentally friendly method for $bioH_2$ production from renewable sources.[1,4] $BioH_2$ generation has been achieved through different routes involving obligate and facultative anaerobes. Dedicated anaerobic bacteria (e.g., *Clostridium* and *Bacteroidetes*) produce volatile fatty acids (VFAs) and $bioH_2$ through glucose degradation. However, dark fermentation is kinetically and thermodynamically limited. Although fermentation provides rapid $bioH_2$ production, accumulation of VFAs and high concentrations of byproducts such as EtOH during fermentation can inhibit $bioH_2$ production, resulting in a lower rate of organic matter conversion to H_2.[5]

To resolve the above issues, many techniques have been proposed, including optimization of process conditions (e.g., pH, organic load, and temperature) and various additives, including activated carbon (AC), biochar (BC), iron(III) oxide (Fe_2O_3), and magnetite, which help buffer the effects of VFA accumulation.[6] Furthermore, the presence of trace elements

Received: January 4, 2022
Accepted: March 9, 2022
Published: March 21, 2022

[e.g., Fe^{2+}, Ni^{+}, Fe^{3+}, and nanoparticles (NPs)] can bring about changes in enzymatic activity and promote the production of extracellular polymers (EPS), thus maintaining sludge granulation.[7] Calcium ions (Ca^{2+}) are mediators that promote EPS production and influence bioH_2 production by facilitating electron transfer and altering EPS composition.[8] Alkaline CaO_2 increases the activity of relevant enzymes and facilitates the release of organic matter from waste sludge.[9] As EPS dissolves, the large amounts of enzymes contained in EPS are also released into the liquid phase, increasing the opportunity for contact with the substrate.[10] The interaction of divalent cations (e.g., Ca^{2+}) with negatively charged material on EPS leads to the release of key enzymes,[11] resulting in the formation of EPS substrates to promote hydrogen production.[11,12] The presence of CO_3^{2} alkalinity mitigates inhibition of the acidic environment by oxygen-containing groups. Furthermore, the hydroxide ion (OH^-) can disrupt the breakdown of refractory organic matter and release suitable substrates for biofuel production.[13]

Hydroxyapatite (HA) NPs free of byproducts, hazardous substances, and impurities were prepared by a coprecipitation method. The synthesized HA NPs with high crystallinity have a high specific surface area and low ion release. The HA obtained after drying and heat treatment can remove water vapor, NH_3, and CO_2 from the precipitate, thus giving hydroxyapatite better biological activity, bioactivity, and biostability. The Ca^{2+} obtained by dissociation in alkaline solution can be used as the calcium source of HA.[14]

In addition, hydroxyapatite has a hexagonal structure comprising a phosphate tetrahedron and a Ca^{2+} site surrounded by OH^-. As a basic metal oxide rich in oxygen groups, it is rarely used in anaerobic dark fermentation. Moreover, HA can be produced from wastes such as phosphogypsum and shellfish, and its crystal structure unit is usually represented as $Ca_{10}(PO_4)_6(OH)_2$.[15] As a new environmentally functional substance, HA has received much attention owing to its biocompatibility.[16] It is often used as an adsorbent to remove heavy metals and dye wastewater from polluted bodies of water.[17]

Additionally, the Ca^{2+} released from HA reacts with soluble phosphorus (PO_4^{3-}) to form a $Ca_3(PO_4)_2$ precipitate; importantly, this enables the reuse of fertilizer from digestate. HA has the potential to be used for dark fermentation, and its end product can be reused as an organic fertilizer or soil conditioner.[17]

Nonetheless, whether the Ca^{2+}, PO_4^{3-}, and OH^- in HA can alter EPS and microbial communities needs to be further investigated to understand the mechanism of dark fermentation. Therefore, studies on the properties of HA in dark fermentation for bioH_2 production, effects of bioH_2 production, and the relationship between HA and microbial communities need further investigation. The aims of this study were (1) to prepare and characterize HA; (2) to study how HA dosage impacts bioH_2 production during dark fermentation; (3) to determine the metabolic pathways and changes in soluble microbial products (SMPs) amended with HA; (4) to explore the results of HA addition on microbial flora in accordance with the phylum, genus, and heat map; and (5) to assess the effects of HA on EPS using the excitation−emission matrix (EEM).

2. MATERIALS AND METHODS

2.1. Fabrication of HA and Characteristics of Inoculated Sludge. Aqueous $Ca(NO_3)_2{\cdot}4H_2O$ (100 mL, 1 M) and $(NH_4)_2HPO_4$ (100 mL, 0.6 M) were prepared separately according to stoichiometry and were slowly mixed by magnetic stirring. The resulting mixture was stirred vigorously for an additional 30 min, and the pH was maintained at 11. The reaction mixture was then dried at 90 °C and stirred for 3 h. After the reaction was completed and cooled, the solution was strained and washed with water and anhydrous EtOH to neutral, and the filtered sample was dried overnight at 80 °C. The sample was then ground and sintered at 10 °C/min and 900 °C for 3 h. Subsequently, the sintered sample was ground and sieved to obtain HA.[18]

The original seed sludge was derived from an up-flow anaerobic sludge bioreactor (UASB) for handling citric acid sewage. To access the dominant fermentation microorganisms, the gathered anaerobic sludge was mixed using glucose (0.5 g) and then cultured for 30 days at 37 °C. Before conducting the bioH_2 generation experiments, the sludge was presoaked at 95 °C for 90 min to restrain the growth of methanogens and to concentrate hydrogen-producing bacteria (HPB). Subsequently, the heated sample was allowed to cool to approximately 37 °C and was incubated for 48 h. The inoculated sludge after the culture had the main parameters including total solids (TS), total organic carbon (TOC), and pH of 7.80 ± 1.67 wt %, 4612.00 ± 195.82 mg/L, and 7.0 ± 0.3, respectively.

One-way analysis of variance (ANOVA) was analyzed to test for significant statistical variations ($p < 0.05$) between the properties of various doses of HA using Origin 2021. All tests were conducted in triplicate.

2.2. Design for Batch Fermentation. BioH_2 production batch experiments were conducted in serum vials with a working volume of 500 mL. Seven gradient levels (20, 100, 200, 400, 800, 1200, and 1600 mg/L) of HA were used to study boiH_2 production, and the group without HA was used as a control. The glucose (10 g/L) and peptone (0.3 g/L) as feeds were added in the reactors, and they were flushed using nitrogen for about 5 min to ensure an anaerobic environment.[19] Prior to the experiments, the pH of the solution was adjusted to 7.0 ± 0.3.[20]

The reactor was subjected to dark fermentation at 37 °C. The fermentation samples were collected every 6 h, and cumulative hydrogen production (CHP) was recorded once every 3 h. SMPs (VFAs and EtOH) were measured with a Shimadzu gas chromatograph along with a flame ionization detector and column (GC-2010). The samples and gases used were collected and sampled as described in a previous study.[19] The hydrogen production rate (HPR) was also calculated based on the standard temperature and pressure (101.3 kPa, 25 °C).[19] The H_2 yield was calculated according to the standard temperature and pressure with eq 1:

$$V_{\text{hydrogen}}(\text{mL, STP}) = V_{\text{hydrogen}}(\text{mL, T}) \times \frac{273}{273 + T} \times \frac{101\,325 - W}{101\,325} \quad (1)$$

where T = 25 °C, and W is the H_2O vapor pressure at 25 °C (Pa).

2.3. Characteristics of HA. The crystal structure of HA was observed using X-ray diffraction (XRD, Bruker, AXS), and measurement curves were recorded at 10° and 80° (2θ). A Brunauer−Emmett−Teller analyzer (BET, Micromeritics, ASAP 2020) was used to assess the pore size, pore volume, and specific area of HA. The structure and crystalline form of

https://doi.org/10.1021/acsomega.2c00059
ACS Omega 2022, 7, 10550−10558

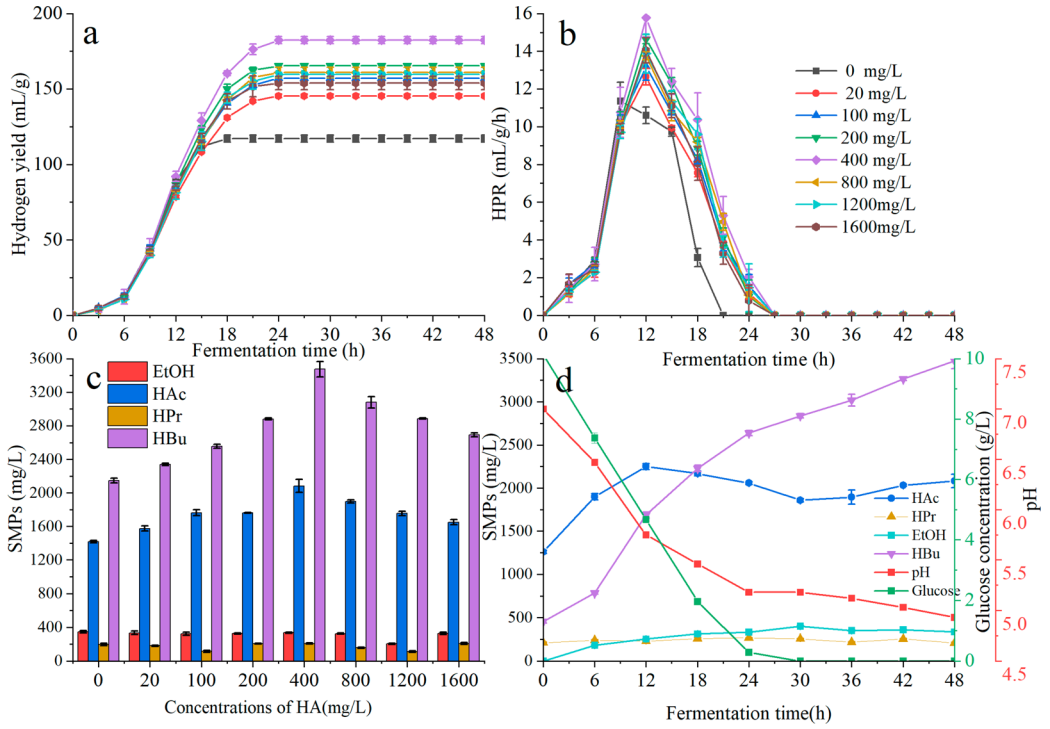

Figure 1. Effects of hydroxyapatite (HA) on bioH_2 production: (a) H_2 yield and (b) HPR. Effects of HA on SMPs or glucose: (c) SMPs and (d) SMPs and glucose with 400 mg/L HA.

HA were observed by transmission electron microscopy (TEM, JEM 2100).

2.4. Collection of Liquid Samples and Analysis. BioH_2 production, expressed in mL/g of glucose, was calculated as the volume of bioH_2 produced per gram of glucose added to the reactor. The samples were passed through a 0.45 μm filtration membrane, and the concentrations of Ca and P in the filtered samples were assayed with inductively coupled plasma (ICP, Optima). The VFAs, pH, 16S rRNA, and EEM were tested in the same way.[21] 16S rRNA gene sequencing was performed using Illumina MiSeq high-throughput sequencing technology for the reactors at the end of H_2 production, and the sequences were resolved at the genus level to analyze HPB diversity.[20] Further, the sludge with HA samples was processed and collected after fermentation. The interactions between HA and HPB were revealed by scanning electron microscopy (SEM, SU8010,) and transmission electron microscopy (TEM, H-7650).

2.5. Significance Test, COD Mass Balance, And Kinetic Modeling. It is critical to assess process kinetics related to anaerobic fermentation reactor design, influencing factors, bioH_2 production potential, and SMPs. Therefore, to determine whether the influence of different dosages of HA on bioH_2 fermentation potential as well as SMPs was statistically significant, ANOVA was performed using Origin 2021 based on the bioH_2 production and SMPs in dark fermentation. According to initial and final COD values as well as equivalent COD for the H_2 produced (8 g COD/g H_2), the COD mass balances were calculated, which were based on eq 2.[19] The maximum hydrogen production (MHP) was assessed using a CHP model.[19] Certain kinetic factors were obtained from Gompertz models, including P_m, R_m, and λ, as shown in eq 3.

$$\text{COD mass balance} = \frac{\text{final COD} + \text{COD}_{H_2}}{\text{initial COD}} \quad (2)$$

$$P(t) = P_m \exp\left\{-\exp\left[\frac{R_m e}{P_m}(\lambda - t) + 1\right]\right\} \quad (3)$$

where P_m is MHP (mL H_2/g glucose), R_m is the maximum H_2 production rate (mL H_2/($g_{glucose}$ h)), $P(t)$ is CHP (mL H_2/$g_{glucose}$) at time t (h), e = 2.718, and λ is the lag time (h). Moreover, the λ, P_m, R_m, and R^2 were evaluated using Origin 2021.

3. RESULTS AND DISCUSSION

3.1. Fabrication of HA. The crystal architecture and surface area of HA are shown in the Supporting Information (Figures S1 and S2). The synthetic HA diffraction pattern was in agreement with that of standard HA (powder diffraction file; PDF, 09-0432). The peaks observed at 2θ angles of 25.8°, 28.1°, 29.0°, 31.7°, 32.2°, 32.8°, 34.0°, and 39.7° can be identified as the (002), (102), (210), (211), (112), (300), (202), and (310) reflections of the HA lattice.

The specific surface area of HA was 4.751 m^2/g. Its adsorption resolution isotherm was Type IV, indicating the presence of voidlike pores on HA, which restricted the absorption of nitrogen over a range of pressures. As P/P_0 increased from 0.9 to 1.0, there was a clear upward trend in the isotherm, owing to the formation of pores resulting from the accumulation of adjacent HA-forming voids.

TEM images show that HA containing calcium and phosphorus was prepared.

3.2. BioH_2 Yield Affected by HA. The bioH_2 and VFAs can be generated by adding glucose to a mixed culture bioreactor. Figure 1 shows the effects of pretreatment on bioH_2 production: (1) CHP for anaerobic dark fermentation

https://doi.org/10.1021/acsomega.2c00059
ACS Omega 2022, 7, 10550−10558

Table 1. Kinetic Parameters of $BioH_2$ Yield from Dark Fermentation Modified with Hydroxyapatite (HA)

HA (mg/L)	0	20	100	200	400	800	1200	1600
P_m (mL/g)	117.73	146.57	158.43	166.73	183.99	162.34	160.89	155.19
R_m (mL/(g h))	16.46	14.02	14.57	15.59	16.92	14.93	15.39	15.41
λ (h)	6.03	6.12	5.98	6.4	6.33	6.33	6.48	6.24
R^2 (%)	99.68	99.87	99.84	99.84	99.84	99.82	99.81	99.77
COD balance (%)	87 ± 0.01	91 ± 0.02	91 ± 0.03	92 ± 0.03	92 ± 0.05	89 ± 0.07	87 ± 0.05	87 ± 0.06
final pH	5.05 ± 0.10	4.97 ± 0.13	5.10 ± 0.11	4.97 ± 0.20	4.93 ± 0.03	4.95 ± 0.10	4.88 ± 0.06	4.84 ± 0.01

reactions amended with HA and (2) HPR exhibited under the dark fermentation reaction with HA.

The $bioH_2$ yield was found to change with the addition of different doses of HA (Figure 1a,b). With the addition of seven gradients of HA, the average $bioH_2$ yields were all higher than those of the control reactor. $BioH_2$ production in the control without HA was 117.03 ± 2.31 mL/g glucose, and the MHP of 182.33 ± 2.41 mL/g glucose could be observed with the inclusion of 400 HA mg/L in the fermentation reaction, which was 55.80% greater than that of the control. The corresponding maximum HPR increased by 38.91%. Several studies have shown that the addition of metal oxides (e.g., CaO and CaO_2) can effectively increase $bioH_2$ productivity, and similar findings have been obtained with HA.[22] This indicated an enhancement of the quantity and quality of short-chain fatty acid production from waste activated sludge using CaO_2 as an additive. HA can maintain the granulation of sludge.[23] The optimal amount of metal ions could alter the morphology of the granular sludge and improve sludge activity, which in turn increases $bioH_2$. Our results indicate that the efficiency of $bioH_2$ generation was improved with the addition of HA (<400 mg/L). A similar observation was obtained in the fermentation of Ca^{2+} granular sludge for $bioH_2$ production.[24] The affinity of HA for microorganisms allows a high enrichment of anaerobic microorganisms, which can provide better conditions for $bioH_2$ production.[25] However, high concentrations of additives can lead to oxidative stress and cell membrane rupture.[26] High doses of HA (>400 mg/L) can thus disrupt the granular sludge structure and create an unfavorable environment for $bioH_2$ operation.[27] The CHP in all reaction groups with HA addition was higher than that in the control group but at different rates of $bioH_2$ production (Figure 1a). Bacterial cell surfaces and EPS are usually negatively charged.[12] With the addition of HA, the Ca^{2+} in HA can connect to the negative charge on EPS, thus forming an EPS substrate and maintaining cellular morphology. The increased EPS secretion promotes the release of hydrogenase-producing enzymes and increases contact with substrates, thus increasing the production of $BioH_2$.[28]

Ca^{2+} increases bacterial abundance by reducing electrostatic repulsion between negatively charged mixed culture bacteria (MCB). The results indicated that moderate amounts of HA increase the rate of $bioH_2$ production from dark fermentation, which could be boosted by enzyme activity, optimization of EPS, and microbial community structure.

3.3. Model-Based Kinetics and Metabolism for $BioH_2$ Generation. As shown in Figure 1a, the $bioH_2$ yield data from anaerobic fermentation were fitted using the modified Gompertz equation. In this study, a one-way ANOVA was performed on data such as H_2 yield under dark fermentation experiments by Origin 2021 to determine whether the effect of HA on dark fermentation was statistically significant. The p-values for all fermentation indicators could be obtained at less than 0.05, indicating that the addition of HA had a significant effect on H_2 yield and SMPs. The kinetic factors λ, R_m, P_m, COD balance, and final pH values are shown in Table 1. The kinetics and analysis of variance can accurately reflect the HA dark fermentation H_2 production. With the increase in HA concentration, there is an adaptation phase for microorganisms. The highest P_m value fitted using the modified Gompertz model was 183.99 mL/g glucose. Its lag time range for fermentation was 5.98−6.48 h. However, there was an adaptation phase for the microorganisms as the HA concentration increased, and there was no significant change in the lag time of the dark fermentation $bioH_2$ production system. The reliability of these data was demonstrated by the fact that COD balance was maintained at 90% during dark fermentation.[29] At the end of dark fermentation for $bioH_2$ production, the final pH dropped to 4.8−5.0 in all reactors. This small change in pH provided opportunities for $bioH_2$ production bacteria to acclimate to the new environment, had few suppressive effects on the microorganisms, and did not limit $bioH_2$ production in this study. The pH values of most production systems were reported to be relatively stable and close to the end pH.[19]

3.4. Impact of HA on $BioH_2$ Fermentation Pathways. SMPs are the main components of $bioH_2$ production from anaerobically fermented organic matter and can be used to evaluate the degradation efficiency of SMPs.[21] Dark fermentation for $bioH_2$ production has been conducted using glucose as a substrate, with EtOH, butyrate (HBu), acetate (HAc), and propionate (HPr) as the main products.[30] Figure 1c depicts the variation in the yield of SMPs in the reactor, which correlates with the biological evolution of $bioH_2$. During dark fermentation, most of the glucose was decomposed, and the accumulation of SMPs varied. Addition of HA significantly promoted the release of soluble metabolites from anaerobically fermented organic matter ($p < 0.05$) (Figure 1c,d). The SMP yield changed with increasing HA content. The optimal dose of HA was 400 mg/L, and the respective concentrations of EtOH, HBu, HAc, and HPr were 335.09 ± 5.16, 3474.72 ± 89.78, 2082.53 ± 76.65, and 207.80 ± 8.58 mg/L (Figure 1c). The concentration of SMPs was 6100.14 ± 109.02 mg/L with the addition of HA, which was 48.35% higher than that of the control.

The change in SMPs produced by dark fermentation in the presence of 400 mg/L HA is presented in Figure 1d. The degradation of glucose was consistent with the production of SMPs over a fermentation time of 6−30 h. Statistical analysis demonstrated p-values less than 0.05, suggesting that the $bioH_2$ generation reactor with added HA had a significant effect on SMPs, HAc, HPr, HBu, and EtOH concentrations. The results showed that anaerobic fermentation reactors with HA addition could improve the $bioH_2$ production rate of the dark fermentation process by providing HA to promote microbial growth and improve microbial activity. In this study, the HAc

https://doi.org/10.1021/acsomega.2c00059
ACS Omega 2022, 7, 10550−10558

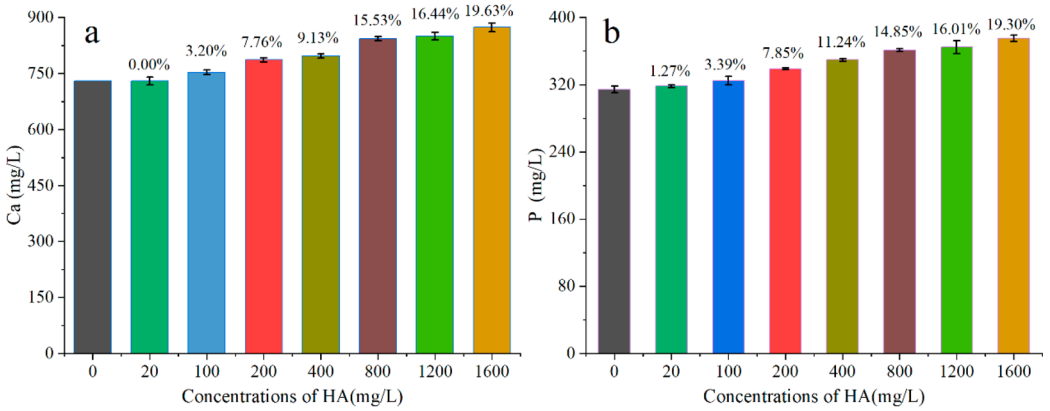

Figure 2. Final concentrations of Ca and P from the dark fermentation system amended with hydroxyapatite (HA): (a) Ca and (b) P (percent releases of Ca and P have been labeled separately on the graph).

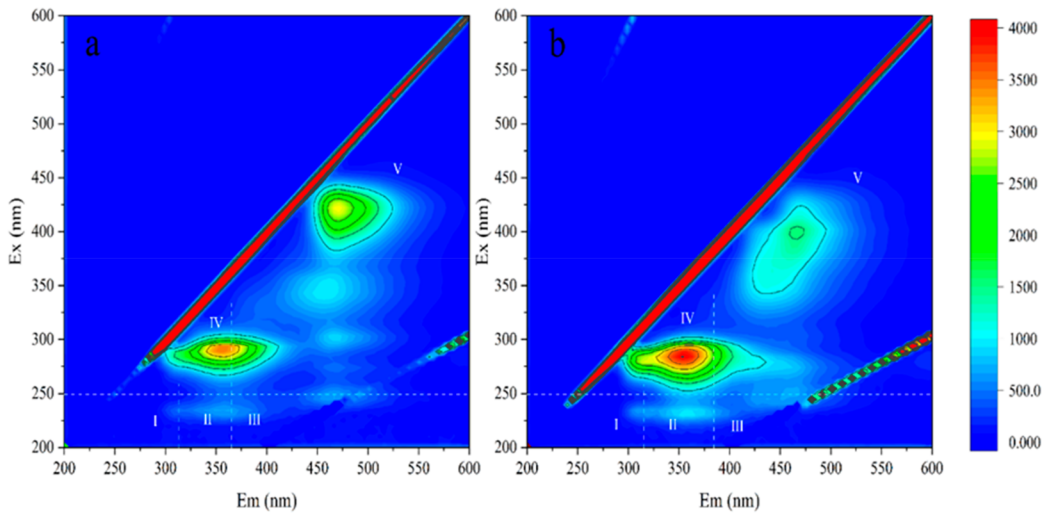

Figure 3. Variation of extracellular polymers (EPS) with hydroxyapatite (HA) dose: (a) 0 mg/L HA and (b) 400 mg/L HA.

and HBu were the dominant acids, suggesting that HAc and HBu production was associated with the dominant HPB groups, *Firmicutes* and *Clostridium butyricum*. As described in eqs 4 and 5, *Clostridium butyricum* was more adapted to bioH_2 yield from HAc- and HBu-type fermentations.[31]

$$C_6H_{12}O_6 + 2H_2O \rightarrow 2CH_3COOH + 2CO_2 + 4H_2$$
$$\Delta G_0 = -206\ \text{KJ/mol} \quad (4)$$

$$C_6H_{12}O_6 \rightarrow CH_3CH_2CH_2COOH + 2CO_2 + 2H_2$$
$$\Delta G_0 = -254\ \text{KJ/mol} \quad (5)$$

The reason is that the HBu-type pathway has lower Gibbs free energy and is thermodynamically more favorable for bioH_2 yield by anaerobic colonies. The molar ratio of HAc to HBu (A/B) was strongly correlated with bioH_2 production. When HA was enriched from 0 to 400 mg/L, A/B decreased from 0.66 to 0.60. Thus, HA addition could enhance the HBu fermentation pathway by increasing the activity and abundance of *Clostridium butyricum*. This phenomenon suggests that the amount of HA added was related to bioH_2 yield. The pH at the end of dark fermentation changed with different doses of HA (Table 1). The pH in all reactors eventually recovered and stabilized in the range 4.8−5.1, which could allow anaerobic fermentation for bioH_2 production.[32]

3.5. Effects of HA on the Morphological Characteristics on HPB. To further investigate the interaction of HA with HPB, the surface of anaerobic bacteria was characterized by SEM with energy spectra for elements such as Ca, P, and C (Figure S3). It was observed that carbon was the basic element of the organisms and was essentially located in the same place on the MCB. In the presence of HA, Ca and P were intensively localized on the bacterial surface in the scan area, and HA was inferred to be attached to the anaerobic bacteria. A previous report also showed that high concentrations of Ca^{2+} increased sludge flocculation with the MHP.[33]

Further, TEM imaging was performed on samples treated with HA after fermentation to observe the interaction between HA and HPB in the dark fermentation system (Figure S4). It was observed that large aggregates of HA were detected on the cell surface.[20,30] Some HA enters the interior of cells and causes damage to the EPS components.[34] The EPS produced by MCB could trap most of the HA, thus interfering with material transfer and affecting electron transport.[35]

HA particles are trapped by EPS and form a membranelike substance that acts as a physical barrier to protect HA, preventing HA particles from attaching to the cell surface or moving into the cell membrane. However, some HA remains capable of perforating the EPS barrier and the cell surface and thus accessing the cell.[5] An addition of 400 mg/L HA revealed

https://doi.org/10.1021/acsomega.2c00059
ACS Omega 2022, 7, 10550−10558

that most cells preserved their proper structure after intrusion, whereas the remainder exhibited destruction of their membranes and intracellular constituents. These characteristics showed variation in the tolerance of cells to HA particles, which affected the morphology of the cell surface and internal structure.

3.6. Effects of HA on the EPS. Figure 2 illustrates the variation of Ca and P elements in the dark fermentation system using HA. The ICP results revealed that the ion concentration increased with increasing HA concentration. With optimal HA (400 mg/L) addition, the concentrations of elements Ca and P reached 796.67 ± 5.77 and 349.67 ± 1.53 mg/L, respectively. The increase in ion concentration during dark fermentation was due to the increased dissolution of HA owing to weak acid conditions. Additionally, the Ca concentration was higher than the P concentration in all reactors. This indicates that the Ca^{2+} released from HA stimulates the activity of hydrolases and proteases.

The influence of HA on the EPS of MCB was evaluated using EEM spectrometry (Figure 3). EEM luminescence spectroscopy can capture specific fluorescence features to differentiate between fluorescent soluble and organic substances in the liquid stage. In this work, EEM was used to characterize extracellular polymers in sludge. Based on previous studies, the soluble organic matter liberated from the fermentation broth can be classified into five types depending on the emission excitation wavelengths (Table 2).[36] In the fermentation reactor with HA addition, it was observed that the intensity of the fluorescence response of the experimental group with HA addition in zone IV was stronger than that in the control group, corresponding to the results of the SMP assay. The fluorescence intensity in the V region was lower than that of the control, and humic acidlike substances were reduced, accelerating their degradation. This may be because Ca^{2+} interacts with EPS to promote the release of hydrolases and proteases, facilitating the hydrolysis of polysaccharides and proteins. Further, the oxygen-rich groups in HA bind to EPS (—COOH, —OH, and —C═O) and weaken the inhibition of anaerobic fermentation.[36] Thus, the presence of HA improved the biodegradability of organic matter and reduced the content of refractory organics. It improves the molecular structure, making the substrate more readily available for microbial uptake and providing a more biodegradable substrate for subsequent fermentation, thus facilitating dark fermentation for bioH_2 production. The remaining dissolved P could also be directly used without treatment as a phosphate fertilizer to promote plant growth.

Table 2. Fluorescence Region Distribution of the EEM

region	Em	Ex	substances
I	200−330	200−250	tyrosine-like protein
II	330−380	200−250	tryptophan-like protein
III	380−500	200−250	fulvic-acid-like organics
IV	200−380	250−280	soluble microbial byproducts
V	380−500	250−400	humic-acid-like organics

3.7. Effects of HA on the Microbial Community. Microbial communities were profiled using high-throughput sequencing to reveal the mechanism by which HA improves bioH_2 fermentation (Figure 4). The results showed that HA addition changed the diversity and abundance of microbial communities. The Simpson diversity of samples with M1 (control, 0 mg/L HA) and M2 (400 mg/L HA) was 0.924 and 0.793, respectively. This result indicates that the addition of HA to dark fermentation reduced bacterial diversity.

The bioH_2 producing phase is accomplished by faster dividing eubacteria, which can distinguish microbial abundance in a shorter period of time. The variation in community structure by phylum and genus is shown in Figure 4. The phylum distribution of MCB in the sludge samples for the control and test groups with 400 mg/L HA is also illustrated. In control trials, Firmicutes, Bacteroidetes, Chloroflexi, Patescibacteria, and Spirochaetae were the main bacterial

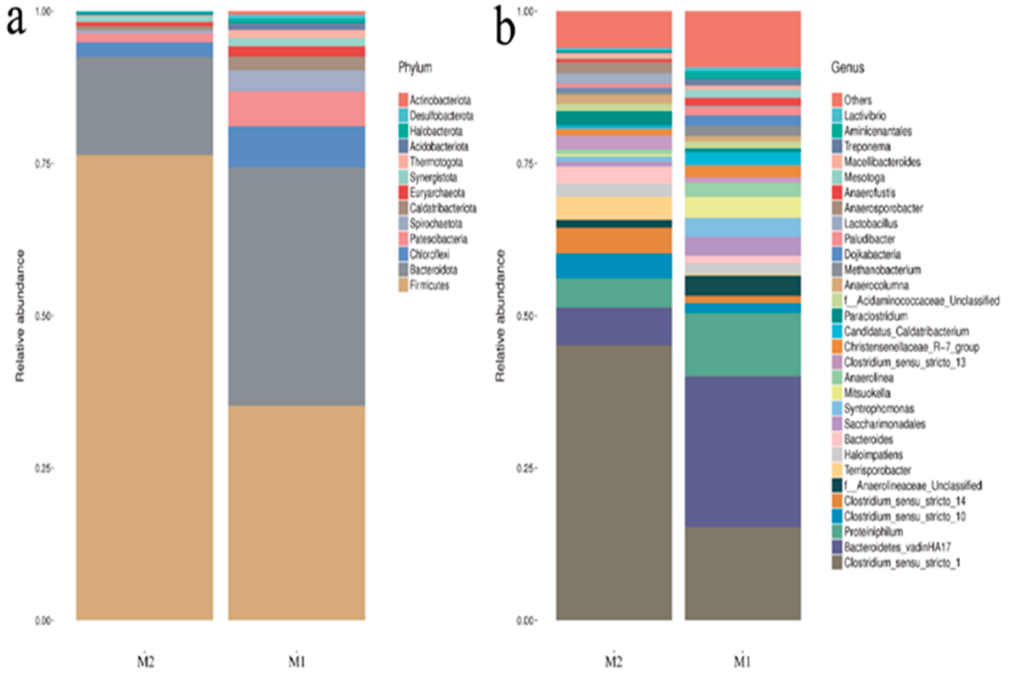

Figure 4. Evolution of the microbial consortium: (a) phylum and (b) genus. M1, 0 mg/L HA; M2, 400 mg/L HA.

https://doi.org/10.1021/acsomega.2c00059
ACS Omega 2022, 7, 10550−10558

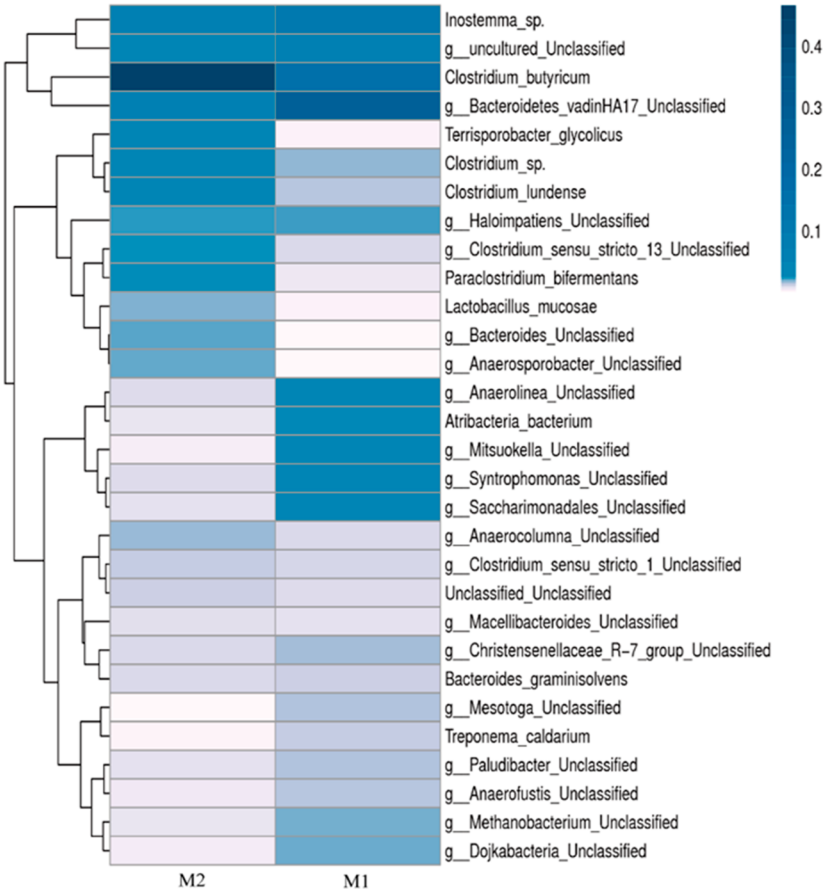

Figure 5. Species-level clustering heat map. M1, 0 mg/L HA; M2, 400 mg/L HA.

phyla, accounting for 35.27%, 39.13%, 6.70%, 5.74%, and 3.49%, respectively, of the total bacterial sequences (Figure 4a). In contrast, in the experiment with 400 mg/L HA, the bacterial community structure comprised Firmicutes, Bacteroidetes, Chloroflexi including Chlorofluorocarbans, and Patescibacteria, accounting for 76.41%, 16.09%, 2.39%, 1.46%, and 0.53%, respectively. Firmicutes and Bacteroidetes remained the dominant bacteria, which is in agreement with previous research.[37] Chloroflexi in the microbiological community during dark fermentation are thought to influence the previous community structure and suppress the development of Proteobacteria and Bacteroidetes. Firmicutes and Bacteroidetes, the main phylogenetic groups, indicated that these phyla have a significant influence on the transformation of organic substances. These results revealed that changes in the abundance of communities were mainly caused by changes in the above-mentioned microorganisms treated with HA. Addition of HA greatly increased the relative abundance of Firmicutes from 35.27% to 76.41%. The results showed that HA increased the enrichment of Firmicutes, which could boost the bioH_2 yield. Firmicutes can produce cellulases, proteases, and many other extracellular enzymes and are specifically associated with the degradation of organic substances, bioH_2 production, and the formation of acids.[38,39] The results indicate that HPB could effectively decompose glucose and generate bioH_2. The reactor with HA facilitated the enrichment and growth of Firmicutes. In particular, the proportion of *Clostridium sensu stricto 1* showed an increase from 15.33% to 45.17% (Figure 4b), which was the most significant change between M1 (control, 0 mg/L HA) and M2 (400 mg/L HA). *Clostridium* is a typical HPB that produces bioH_2 from diverse organic substrates such as hemicellulose, cellulose, starch, sucrose, and glucose. Under analogous pretreatment terms, *Clostridium* has also been found as the key species in other dark fermentations, such as in bioH_2 production from mixed cultures pretreated with radiation and acid.[40] The structure of the microbial community evolved in bioH_2 generation revealed that *Clostridium sensu stricto 1* was directly related to bioH_2 production.[41] Bacteroidetes, Proteobacteria, and Chloroflexi species were present symbiotically in the community, whereas Firmicutes evolved independently and rarely interacted with other bacteria, degrading complex organic matter into small molecules. This partly facilitated its successful increase in dark fermentation for bioH_2 production, gradually gaining dominance in the microbial community.[42]

Further, a higher proportion of bacterial were found to belong to Firmicutes, whose abundance accounts for 72%.[39] In the present study, a high percentage of HBu was achieved by the addition of HA. *Clostridium butyrium* also increased significantly, as shown in Figure 5. In fact, *Clostridium butyricum* produced only HBu. Therefore, HBu as a product of *Clostridium butyricum* indicated that H_2 production is more adapted to HBu-type fermentation in the presence of HA.

Therefore, Firmicutes, *Clostridium sensu stricto 1*, and *Clostridium butyrium* might be closely related to the production of HBu during dark fermentation. Therefore, enrichment of Firmicutes and *Clostridium* is probably the primary cause for enhanced bioH_2 production by HA addition.

Although HA could be employed to enable high bioH_2 yields, the probable mechanisms are mostly related to HA

https://doi.org/10.1021/acsomega.2c00059
ACS Omega 2022, 7, 10550−10558

concentration and microbial diversity.[43] Its possible mechanisms are as follows: (1) Ca and P elements enhance the activities of HPB and optimize the microbial community structure, and (2) HA enriches the dominant HPB with Firmicutes (76.41%) and *Clostridium sensu stricto 1* (45.17%) at an optimal concentration of 400 mg/L, which enhances bioH_2 production. Future efforts are required to assess the sustainability and feasibility of modified HA-mixed fermentation for bioH_2 production from complex organic compounds.

4. CONCLUSION

The effects of different doses of HA on bioH_2 were investigated using dark fermentation. The results showed that the highest bioH_2 yield was obtained with 400 mg/L of HA addition, which was 55.80% higher than that of the control group. HA addition enhanced the bioH_2 yield of dark fermentation and increased the abundance of HPB with Firmicutes and *Clostridium sensu stricto 1* being dominant. HA contributes to HBu-type fermentation, maintains pH balance, and promotes enzyme activity. However, excess HA (>800 mg/L) reduced the bioH_2 yield owing to the higher Ca^{2+} concentration released from HA.

■ ASSOCIATED CONTENT

Supporting Information

The Supporting Information is available free of charge at https://pubs.acs.org/doi/10.1021/acsomega.2c00059.

Additional figures including hydroxyapatite material characterization and interaction of added hydroxyapatite with fermented sludge (PDF)

■ AUTHOR INFORMATION

Corresponding Authors

Weifang Dong − *School of Environmental Science and Engineering, Qilu University of Technology (Shandong Academy of Science), Jinan 250353, China*; Email: dwf@qlu.edu.cn

Lihua Zang − *School of Environmental Science and Engineering, Qilu University of Technology (Shandong Academy of Science), Jinan 250353, China; Jilin Meihua Amino Acid Co., Ltd., Baicheng 137000, China*; orcid.org/0000-0002-0814-3001; Email: zlh@qlu.edu.cn

Authors

Haoe Mo − *School of Environmental Science and Engineering, Qilu University of Technology (Shandong Academy of Science), Jinan 250353, China*

Na Wang − *School of Environmental Science and Engineering, Qilu University of Technology (Shandong Academy of Science), Jinan 250353, China*

Zhongmin Ma − *School of Environmental Science and Engineering, Qilu University of Technology (Shandong Academy of Science), Jinan 250353, China*

Jishi Zhang − *School of Environmental Science and Engineering, Qilu University of Technology (Shandong Academy of Science), Jinan 250353, China*; orcid.org/0000-0003-0054-2726

Jinlong Zhang − *Jilin Meihua Amino Acid Co., Ltd., Baicheng 137000, China*

Lu Wang − *Jilin Meihua Amino Acid Co., Ltd., Baicheng 137000, China*

Complete contact information is available at: https://pubs.acs.org/10.1021/acsomega.2c00059

Notes

The authors declare no competing financial interest.

■ ACKNOWLEDGMENTS

This work was supported by the Integration of Science, Education and Industry Innovation Pilot Project of Qilu University of Technology (Shandong Academy of Sciences) (2020KJC-ZD12).

■ ABBREVIATIONS

HA, hydroxyapatite; bioH_2, biohydrogen; H_2, hydrogen; SMPs, soluble microbial products; EtOH, ethanol; COD, chemical oxygen demand; VFAs, volatile fatty acids; AC, activated carbon; BC, biochar; Fe_2O_3, iron(III) oxide; NPs, nanoparticles; EPS, extracellular polymers; Ca^{2+}, calcium ions; −OH, hydroxyl; PO_4^{3-}, phosphorus; SMPs, soluble microbial products; EEM, excitation−emission matrix; UASB, up-flow anaerobic sludge bioreactor; HPB, hydrogen-producing bacteria; TS, total solids; TOC, total organic carbon; ANOVA, analysis of variance; XRD, X-ray diffraction; BET, Brunauer−Emmett−Teller; TEM, transmission electron microscopy; ICP, inductively coupled plasma; SEM, scanning electron microscopy; TEM, transmission electron microscopy; MHP/MHY, maximum hydrogen production; CHP, cumulative hydrogen production; HPR, hydrogen production rate; MCB, mixed culture bacteria; HAc, acetate; HPr, propionate; HBu, butyrate

■ REFERENCES

(1) Paris, B.; Papadakis, G.; Janssen, R.; Rutz, D. Economic analysis of advanced biofuels, renewable gases, electrofuels and recycled carbon fuels for the Greek transport sector until 2050. *Renewable and Sustainable Energy Reviews* **2021**, *144*, 111038.

(2) Anejionu, O. C. D.; Di Lucia, L.; Woods, J. Geospatial modelling of environmental and socioeconomic impacts of large-scale production of advanced biofuel. *Biomass Bioenergy* **2020**, *142*, 105789.

(3) Salem, A. H.; Mietzel, T.; Brunstermann, R.; Widmann, R. Two-stage anaerobic fermentation process for bio-hydrogen and bio-methane production from pre-treated organic wastes. *Bioresour. Technol.* **2018**, *265*, 399−406.

(4) Wang, Y.; Wang, Z.; Zhang, Q.; Li, G.; Xia, C. Comparison of bio-hydrogen and bio-methane production performance in continuous two-phase anaerobic fermentation system between co-digestion and digestate recirculation. *Bioresour. Technol.* **2020**, *318*, 124269.

(5) Cheng, J.; Li, H.; Ding, L.; Zhou, J.; Song, W.; Li, Y.-Y.; Lin, R. Improving hydrogen and methane co-generation in cascading dark fermentation and anaerobic digestion: The effect of magnetite nanoparticles on microbial electron transfer and syntrophism. *Chem. Eng. J.* **2020**, *397*, 125394.

(6) Zhang, J.; Zhao, W.; Zhang, H.; Wang, Z.; Fan, C.; Zang, L. Recent achievements in enhancing anaerobic digestion with carbon-based functional materials. *Bioresour. Technol.* **2018**, *266*, 555−567.

(7) Zagrodnik, R.; Duber, A.; Seifert, K. Hydrogen production during direct cellulose fermentation by mixed bacterial culture: The relationship between the key process parameters using response surface methodology. *J. Cleaner Prod.* **2021**, *314*, 127971.

(8) Ma, H.; Guo, C.; Yao, M.; Wu, M.; Wang, Z.; Wang, S. Calcium ions affect sludge digestion performance via changing extracellular polymeric substances in anaerobic bioreactor. *Biomass Bioenergy* **2020**, *137*, 105548.

(9) Wang, D.; Zhang, D.; Xu, Q.; Liu, Y.; Wang, Q.; Ni, B.-J.; Yang, Q.; Li, X.; Yang, F. Calcium peroxide promotes hydrogen production

from dark fermentation of waste activated sludge. *Chem. Eng. J.* **2019**, *355*, 22−32.
(10) Yang, J.; Zhang, J.; Zhang, J.; Zhang, J.; Yang, Y.; Zang, L. Roles of calcium-containing alkali materials on dark fermentation and anaerobic digestion: A systematic review. *Int. J. Hydrogen Energy* **2021**, *46* (78), 38645−38662.
(11) Li, J.; Hao, X.; van Loosdrecht, M. C. M.; Liu, R. Relieving the inhibition of humic acid on anaerobic digestion of excess sludge by metal ions. *Water Res.* **2021**, *188*, 116541.
(12) Sobeck, D. C.; Higgins, M. J. Examination of three theories for mechanisms of cation-induced bioflocculation. *Water Res.* **2002**, *36* (3), 527−538.
(13) Xu, Y.; Lu, Y.; Zheng, L.; Wang, Z.; Dai, X. Perspective on enhancing the anaerobic digestion of waste activated sludge. *J. Hazard. Mater.* **2020**, *389*, 121847.
(14) Karampour, H.; Parsa, M. A.; Moghadam, A. H.; Pourhasan, B.; Ashiri, R. Facile solution-based synthesis of impurity-free hydroxyapatite nanocrystals at ambient conditions. *Journal of Materials Research and Technology* **2022**, *16*, 656−674.
(15) Zhang, D.; Luo, H.; Zheng, L.; Wang, K.; Li, H.; Yi, W.; Feng, H. J. J. o. H. M. Utilization of waste phosphogypsum to prepare hydroxyapatite nanoparticles and its application towards removal of fluoride from aqueous solution. *J. Hazard. Mater.* **2012**, *241*−*242*, 418−426.
(16) Bharti, A.; Singh, S.; Meena, V. K.; Goyal, N. Structural Characterization of Silver-Hydroxyapatite Nanocomposite: A Bone Repair Biomaterial. *Mater. Today: Proc.* **2016**, *3* (6), 2113−2120.
(17) Fan, Y.; Wu, Q.; Bao, B.; Cao, Y.; Zhang, S.; Cui, H. Ferrihydrite reduces the bioavailability of copper and cadmium and phosphorus release risk in hydroxyapatite amended soil. *J. Environ. Chem. Eng.* **2021**, *9* (6), 106756.
(18) Mobasherpour, I.; Heshajin, M. S.; Kazemzadeh, A.; Zakeri, M. Synthesis of nanocrystalline hydroxyapatite by using precipitation method. *J. Alloys Compd.* **2007**, *430* (1), 330−333.
(19) Zhao, W.; Zhang, J.; Zhang, H.; Yang, M.; Zang, L. Comparison of mesophilic and thermophilic biohydrogen production amended by nickel-doped magnetic carbon. *J. Cleaner Prod.* **2020**, *270*, 122730.
(20) Zhang, J.; Zhao, W.; Yang, J.; Li, Z.; Zhang, J.; Zang, L. Comparison of mesophilic and thermophilic dark fermentation with nickel ferrite nanoparticles supplementation for biohydrogen production. *Bioresour. Technol.* **2021**, *329*, 124853.
(21) Cao, X.; Zhao, L.; Dong, W.; Mo, H.; Ba, T.; Li, T.; Guan, D.; Zhao, W.; Wang, N.; Ma, Z.; et al. Revealing the mechanisms of alkali-based magnetic nanosheets enhanced hydrogen production from dark fermentation: Comparison between mesophilic and thermophilic conditions. *Bioresour. Technol.* **2022**, *343*, 126141.
(22) Li, Y.; Wang, J.; Zhang, A.; Wang, L. Enhancing the quantity and quality of short-chain fatty acids production from waste activated sludge using CaO_2 as an additive. *Water Res.* **2015**, *83*, 84−93.
(23) Liang, L.; Luo, J.; Xiao, X.; Wang, J.; Hong, M.; Deng, C.; Li, Y.-Y.; Liu, J. Granular activated carbon promoting re-granulation of anammox-hydroxyapatite granules for stable nitrogen removal at low phosphate concentration. *Sci. Total Environ.* **2022**, *805*, 150359.
(24) Chang, F.-Y.; Lin, C.-Y. J. W. s. technology. Calcium effect on fermentative hydrogen production in an anaerobic up-flow sludge blanket system. *Water Sci. Technol.* **2006**, *54* (9), 105−112.
(25) Sun, S.; Gao, M.; Wang, Y.; Qiu, Q.; Han, J.; Qiu, L.; Feng, Y. Phosphate removal via biological process coupling with hydroxyapatite crystallization in alternating anaerobic/aerobic biofilter reactor. *Bioresour. Technol.* **2021**, *326*, 124728.
(26) Wang, D.; Chen, Y. J. C. r. i. b. Critical review of the influences of nanoparticles on biological wastewater treatment and sludge digestion. *Water Res.* **2016**, *36* (5), 816−828.
(27) Yu, H. Q.; Tay, J. H.; Fang, H. H. P. The roles of calcium in sludge granulation during uasb reactor start-up. *Water Res.* **2001**, *35* (4), 1052−1060.
(28) Zhang, J.; Li, W.; Yang, J.; Li, Z.; Zhang, J.; Zhao, W.; Zang, L. Cobalt ferrate nanoparticles improved dark fermentation for hydrogen evolution. *J. Cleaner Prod.* **2021**, *316*, 128275.
(29) Gupta, M.; Gomez-Flores, M.; Nasr, N.; Elbeshbishy, E.; Hafez, H.; Hesham El Naggar, M.; Nakhla, G. Performance of mesophilic biohydrogen-producing cultures at thermophilic conditions. *Bioresour. Technol.* **2015**, *192*, 741−747.
(30) Zhang, P.; Xu, X.-Y.; Zhang, X.-L.; Zou, K.; Liu, B.-Z.; Qing, T.-P.; Feng, B. Nanoparticles-EPS corona increases the accumulation of heavy metals and biotoxicity of nanoparticles. *J. Hazard. Mater.* **2021**, *409*, 124526.
(31) Yang, J.; Zhang, J.; Li, Z.; Zhang, J.; Zhao, L.; Zang, L. Calcium-doped carbon fabrication for improving bioH_2 and bioCH_4 production. *Int. J. Hydrogen Energy* **2021**, *46* (41), 21348−21358.
(32) Cruz Viggi, C.; Rossetti, S.; Fazi, S.; Paiano, P.; Majone, M.; Aulenta, F. J. E. s. technology. Magnetite particles triggering a faster and more robust syntrophic pathway of methanogenic propionate degradation. *Environ. Sci. Technol.* **2014**, *48* (13), 7536−7543.
(33) Chen, Z.; Zhang, W.; Wang, D.; Ma, T.; Bai, R.; Yu, D. Enhancement of waste activated sludge dewaterability using calcium peroxide pre-oxidation and chemical re-flocculation. *Water Res.* **2016**, *103*, 170−181.
(34) Zakaria, B. S.; Dhar, B. R. Changes in syntrophic microbial communities, EPS matrix, and gene-expression patterns in biofilm anode in response to silver nanoparticles exposure. *Sci. Total Environ.* **2020**, *734*, 139395.
(35) Vu, M. T.; Noori, M. T.; Min, B. Conductive magnetite nanoparticles trigger syntrophic methane production in single chamber microbial electrochemical systems. *Bioresour. Technol.* **2020**, *296*, 122265.
(36) Chen, Y.; Yao, H.; Kong, F.; Tian, H.; Meng, G.; Wang, S.; Mao, X.; Cui, X.; Hou, X.; Shi, J. V_2C MXene synergistically coupling FeNi LDH nanosheets for boosting oxygen evolution reaction. *Appl. Catal., B* **2021**, *297*, 120474.
(37) Wan, J.; Jing, Y.; Zhang, S.; Angelidaki, I.; Luo, G. Mesophilic and thermophilic alkaline fermentation of waste activated sludge for hydrogen production: Focusing on homoacetogenesis. *Water Res.* **2016**, *102*, 524−532.
(38) Levén, L.; Eriksson, A. R.; Schnürer, A. J. F. m. e. Effect of process temperature on bacterial and archaeal communities in two methanogenic bioreactors treating organic household waste. *FEMS Microbiol. Ecol.* **2007**, *59* (3), 683−693.
(39) Lim, J. W.; Chiam, J. A.; Wang, J.-Y. Microbial community structure reveals how microaeration improves fermentation during anaerobic co-digestion of brown water and food waste. *Bioresour. Technol.* **2014**, *171*, 132−138.
(40) Yin, Y.; Wang, J. Changes in microbial community during biohydrogen production using gamma irradiated sludge as inoculum. *Bioresour. Technol.* **2016**, *200*, 217−222.
(41) Yang, G.; Yin, Y.; Wang, J. Microbial community diversity during fermentative hydrogen production inoculating various pre-treated cultures. *Int. J. Hydrogen Energy* **2019**, *44* (26), 13147−13156.
(42) Zhou, L.; Gao, Y.; Yu, K.; Zhou, H.; De Costa, Y. G.; Yi, S.; Zhuang, W.-Q. Microbial community in in-situ waste sludge anaerobic digestion with alkalization for enhancement of nutrient recovery and energy generation. *Bioresour. Technol.* **2020**, *295*, 122277.
(43) Kumar, G.; Mathimani, T.; Rene, E. R.; Pugazhendhi, A. Application of nanotechnology in dark fermentation for enhanced biohydrogen production using inorganic nanoparticles. *Int. J. Hydrogen Energy* **2019**, *44* (26), 13106−13113.

https://doi.org/10.1021/acsomega.2c00059
ACS Omega 2022, 7, 10550−10558